ELSEVIER

Journal of Chromatography A, 915 (2001) 1–13

JOURNAL OF CHROMATOGRAPHY A

www.elsevier.com/locate/chroma

A hybrid of exponential and gaussian functions as a simple model of asymmetric chromatographic peaks

Kevin Lan, James W. Jorgenson*

Department of Chemistry, University of North Carolina at Chapel Hill, Venable Hall, CB 3290, Chapel Hill, NC 27599-3290, USA

Received 8 August 2000; received in revised form 26 January 2001; accepted 26 January 2001

Abstract

A hybrid of exponential and Gaussian functions is developed as a model of asymmetric peak profiles. This exponential-Gaussian hybrid function (EGH) is mathematically simple, numerically stable, and its parameters are readily determined by making graphical measurements and applying simple equations. Furthermore, the statistical moments of the EGH function can be accurately approximated (within±0.15% error) at any level of asymmetry using formulae that are easily programmed into a computer. These features of the EGH make it very easy to implement by most chromatographers. The EGH serves as a useful alternative to the exponentially modified Gaussian (EMG) for modeling slightly asymmetric peaks since the two models produce nearly the same profile at relatively low asymmetries. The EGH also serves as an addition to the extensive list of alternative models that are sometimes better than the EMG at describing highly asymmetric peaks. A comparison between EMG and EGH curves at various asymmetries is made by analysis of toluene, phenylalanine, and pyridine on a reversed-phase liquid chromatographic system.

Keywords: Peak profiles; Exponential-Gaussian hybrid function

1. Introduction

Although the Gaussian function is frequently used to describe the ideal shape of chromatographic peaks, such profiles are rarely observed experimentally. Of the many processes [1–5] that lead to peak distortion, the most pronounced effect often arises from a single exponential-decay-like phenomenon, e.g. a poorly swept extra-column volume or a slow rate of mass transfer. In such cases, the profile of the peak may be better described by a Gaussian function $f_{gau}(t)$ that has been modified in some manner so that it is closer in character to a truncated exponential function $f_{exp}(t)$:

$$f_{gau}(t) = H \exp\left(\frac{-(t-t_R)^2}{2\sigma_g^2}\right) \quad (1)$$

$$f_{exp}(t) = \begin{cases} H \exp\left(\dfrac{-(t-t_R)}{\tau}\right), & \tau(t-t_R) > 0, \\ 0, & \tau(t-t_R) \le 0 \end{cases} \quad (2)$$

where H is the peak height (magnitude of the peak maximum), t_R is the retention time (time of the peak

*Corresponding author. Tel.: +1-919-966-5071; fax: +1-919-962-1381.

E-mail address: jj@unc.edu (J.W. Jorgenson).

0021-9673/01/$ – see front matter
PII: S0021-9673(01)00594-5

maximum), σ_g is the standard deviation of the peak, and τ is the time constant of exponential decay.

There are numerous models of asymmetric peaks described in literature, such as the exponentially modified Gaussian [3,6–8], polynomially modified Gaussian [9], Edgeworth–Cramer series [10], Chesler–Cram [11], bi-Gaussian [12], Poisson distribution [12], Fraser–Suzuki [13], log-normal distribution [14], exponentially modified non-Gaussian functions [15], generalized exponential [16], and Harhoff–van der Linde [17]. Of these models, exponentially modified Gaussian function (EMG, Fig. 1) is vastly the most popular. The EMG is derived by convolution of the Gaussian function with a truncated exponential where $t_R = 0$ and $H = 1/\tau$. When $\tau > 0$, the EMG $f_{emg}(t)$ is closely approximated by [18]:

$$f_{emg}(t) = \frac{M_0}{2\tau}\exp\left(\frac{\sigma_g^2}{2\tau^2} - \frac{t - t_g}{\tau}\right) \times \operatorname{erfc}\left(\frac{1}{\sqrt{2}}\left(\frac{\sigma_g}{\tau} - \frac{t - t_g}{\sigma_g}\right)\right) \quad (3)$$

where M_0 is the peak area (zeroth statistical moment), τ is the time constant of the precursor exponential, σ_g is the standard deviation of the precursor Gaussian, and t_g is the retention time of the precursor Gaussian (the symbol t_g is used is place of t_R because it does not correspond to the time of the EMG maximum). The EMG approaches the Gaussian profile as $\tau \to 0$, and it likewise approaches the truncated exponential profile as $\sigma_g \to 0$:

$$\lim_{\tau \to 0} f_{emg}(t) = f_{gau}(t) \quad (4)$$

$$\lim_{\sigma_g \to 0} f_{emg}(t) = f_{exp}(t) \quad (5)$$

The EMG generally provides a very good fit for a broad range of peaks [19]. Significant deviations are generally found only in highly asymmetric peaks [19], which are instead more effectively modeled using one of the other models listed previously.

The EMG has the convenient property that its statistical moments are expressed in simple terms of its parameters [20]:

$$M_1 = t_g + \tau \quad (6)$$

$$\bar{M}_2 = \sigma_g^2 + \tau^2 \quad (7)$$

$$\bar{M}_3 = 2\tau^3 \quad (8)$$

$$\bar{M}_4 = 3\sigma_g^4 + 6\sigma_g^2\tau^2 + 9\tau^4 \quad (9)$$

Unfortunately, none of the parameters (M_0, t_g, σ_g, τ) of the EMG can be deduced easily from graphical measurements. Approximations have been developed [21–23] that allow for the calculation of the temporal parameters (t_g, σ_g, τ) based on measurements of the retention time and the asymmetry quantities $A_{0.1}$ and $B_{0.1}$, which are the absolute horizontal distances from the vertical line containing the peak maximum to the leading ($A_{0.1}$) and trailing ($B_{0.1}$) edges measured at 0.1 (10%) of the peak height (Fig. 1, $\theta = \pi/4$). Other approximate methods of determining the statistical moments and parameters of the EMG are described in Refs. [24–26].

Although the EMG function is widely used and accepted, there are some instances in which an alternative to the EMG is needed. For example, at very low asymmetries, the calculation of the EMG becomes numerically unstable [19] because it relies upon the relative accuracy of extremely small values from the complementary error function. Unfortunately, the peaks of low asymmetry are the most common, and they are the peaks that are best described by the EMG [19]. It would thus be useful to have a similarly shaped, numerically stable alternative to the EMG at low asymmetries. At higher asymmetries, the EMG often does not describe the shape of an experimental peak very well [9,19]. In

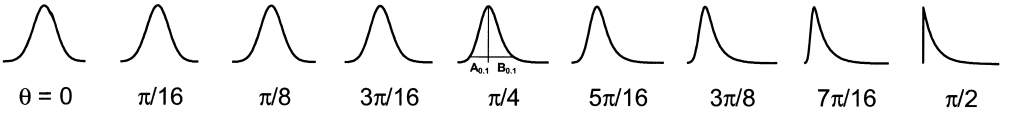

Fig. 1. Exponentially modified Gaussian (EMG) profiles ranging from no asymmetry ($\theta = 0$) to extreme asymmetry ($\theta = \pi/2$). Each profile has the same peak height and second normalized central moment, and each profile is truncated to eliminate ordinate values less than 1/1024 of the peak height.

these cases, alternative models, such as those listed previously, may be better suited for describing the peak shape. Both of these roles can be served by the exponential-Gaussian hybrid (EGH) function, which is detailed in this manuscript.

2. Theory

2.1. Exponential-Gaussian Hybrid

The Gaussian and truncated exponential functions may be restated in the following forms:

$$f_{\text{gau}}(t) = \begin{cases} H \exp\left(\dfrac{-(t-t_{\text{R}})^2}{2\sigma_g^2}\right), & 2\sigma_g^2 > 0, \\ 0, & 2\sigma_g^2 \le 0 \end{cases} \tag{10}$$

$$f_{\text{exp}}(t) = \begin{cases} H \exp\left(\dfrac{-(t-t_{\text{R}})^2}{\tau(t-t_{\text{R}})}\right), & \tau(t-t_{\text{R}}) > 0, \\ 0, & \tau(t-t_{\text{R}}) \le 0 \end{cases} \tag{11}$$

The Gaussian and truncated exponential functions are very similar when expressed in this format; their only difference is the denominator of the argument in the exponential function. Note that both functions are nullified when the denominator of the exponential argument is less than or equal to zero. By combining the denominators in each argument, we produce the exponential-Gaussian hybrid function $f_{\text{egh}}(t)$ (Fig. 2):

$$f_{\text{egh}}(t) \equiv \begin{cases} H \exp\left(\dfrac{-(t-t_{\text{R}})^2}{2\sigma_g^2 + \tau(t-t_{\text{R}})}\right), & 2\sigma_g^2 + \tau(t-t_{\text{R}}) > 0, \\ 0, & 2\sigma_g^2 + \tau(t-t_{\text{R}}) \le 0 \end{cases} \tag{12}$$

where H is the magnitude of the peak maximum, t_{R} is the retention time, σ_g is the standard deviation of the precursor Gaussian, and τ is the time constant of the precursor exponential. Like the EMG, the EGH also has the important property that its profile approaches a Gaussian profile as $\tau \to 0$, and it approaches a truncated exponential profile as $\sigma_g \to 0$:

$$\lim_{\tau \to 0} f_{\text{egh}}(t) = f_{\text{gau}}(t) \tag{13}$$

$$\lim_{\sigma_g \to 0} f_{\text{egh}}(t) = f_{\text{exp}}(t) \tag{14}$$

2.2. Determination of Parameters for the EGH

An important practical feature of the EGH is that its parameters are easily determined from graphical information. The retention time t_{R} and the peak height H constitute the coordinate of the peak maximum, and the variance σ_g^2 of the precursor Gaussian and time constant τ of the precursor truncated exponential can be determined by (Appendix A):

$$\sigma_g^2 = \frac{-1}{2 \ln \alpha}(B_\alpha A_\alpha) \tag{15}$$

$$\tau = \frac{-1}{\ln \alpha}(B_\alpha - A_\alpha) \tag{16}$$

where A_α and B_α are the general forms of $A_{0.1}$ and $B_{0.1}$ where α denotes the fraction of the peak height at which the distances are measured. The relationships given in (15) and (16) are analytically exact for pure EGH curves. Note that σ_g^2 is proportional to the product of B_α and A_α, and that τ is proportional the difference between B_α and A_α.

2.3. Determination of Statistical Moments for the EGH

In contrast to the EMG, the statistical moments of the EGH are relatively difficult to calculate from its parameters. The authors are unaware of any exact

Fig. 2. Exponential-Gaussian hybrid (EGH) profiles ranging from no asymmetry ($\theta = 0$) to extreme asymmetry ($\theta = \pi/2$). Each profile has the same peak height and second normalized central moment, and each profile is truncated to eliminate ordinate values less than 1/1024 of the peak height.

expressions for the statistical moments of the EGH that can be evaluated. Nonetheless, the statistical moments of a pure EGH curve can be calculated to arbitrary accuracy using numerical integration [26]:

$$M_0 = \int_{-\infty}^{\infty} f_{\mathrm{egh}}(t)\,\mathrm{d}t \tag{17}$$

$$M_1 = \frac{1}{M_0}\int_{-\infty}^{\infty} t f_{\mathrm{egh}}(t)\,\mathrm{d}t \tag{18}$$

$$\bar{M}_n = \frac{1}{M_0}\int_{-\infty}^{\infty} (t - M_1)^n f_{\mathrm{egh}}(t)\,\mathrm{d}t \tag{19}$$

In practice, the determination of statistical moments by numerical integration has a few minor disadvantages. Numerical integration is relatively slow since it involves a large number of repeated computations. This issue may be important when a large number of peaks need to be processed. Furthermore, the accuracy of results given by basic numerical integration algorithms (such as fourth-order Runge-Kutta) is usually unknown. In these cases, the only way to estimate the potential error of the result is to repeat the numerical integration using a smaller step size, which is even more time-consuming. Finally, numerical integration can be somewhat difficult to program for those without a computing background.

An alternative to numerical integration is to use approximate expressions of the statistical moments. To develop these approximations, we generalize a strategy that is commonly used to estimate EMG moments [21,23,24]. Consider a set of EGH curves that have the same level of asymmetry $|\tau|/\sigma_g$. Within this set, the zeroth statistical moment M_0 (peak area) of a curve is proportional to the peak height H and the peak width w:

$$M_0 = Hw \cdot \epsilon_0 \tag{20}$$

where ϵ_0 is a proportionality constant. Since σ_g and $|\tau|$ are temporal parameters that describe the width of a peak, either can be used as a measure of peak width at a fixed level of asymmetry. (Note that peak width, σ_g, and τ all have units of time. See Appendix B.) Moreover, because σ_g and $|\tau|$ are proportional to each other at a fixed level of asymmetry, any expression that is first order overall with respect to σ_g and $|\tau|$ can also be used as a measure of peak width. For example, one possible expression for the zeroth statistical moment is:

$$M_0 = H\left(\sigma_g\sqrt{\frac{\pi}{8}} + |\tau|\right)\epsilon_0 \tag{21}$$

For Eq. (21) to be generally applicable at any level of asymmetry, the proportionality constant ϵ_0 must be expressed as a function of $|\tau|/\sigma_g$. Although this relationship cannot be determined analytically, a fit of numerically calculated values of ϵ_0 can provide an approximate solution. A minor complication to this approach is that the fit of ϵ_0 must cover all levels of asymmetry $|\tau|/\sigma_g$, and it is difficult to fit a function over an infinite domain. This issue was resolved previously [27] by using the arc tangent function to map all levels of asymmetry to a finite range. A similar approach is used here:

$$\theta \equiv \arctan\left(\frac{|\tau|}{\sigma_g}\right) \tag{22}$$

where θ is the absolute bounded asymmetry. Absolute bounded asymmetries have values between zero (Gaussian) and $\pi/2$ (truncated exponential), and they can be used efficiently in a polynomial fit of ϵ_0:

$$\epsilon_0 \approx \sum_{i=0}^{m} a_i\theta^i = a_0 + a_1\theta + a_2\theta^2 + a_3\theta^3 + \cdots a_m\theta^m \tag{23}$$

where m is the order of the polynomial, and a_i is the coefficient of the ith order term in the polynomial. Once an appropriate fit of ϵ_0 is determined, Eq. (21) can be used as a general approximation of the zeroth statistical moment of the EGH. The strategy described above is based on factoring the statistical moment into two independent parts: a factor of scale (e.g., Hw in Eq. (20)) that accounts for the size of the peak, and a factor of asymmetry (e.g., ϵ_0 in Eq. (20)) that accounts for the shape of the peak. This approach can also be applied to higher order moments (Appendix C):

$$M_1 - t_{\mathrm{R}} = \tau\epsilon_1 \tag{24}$$

$$\bar{M}_2 = \left(\sigma_g^2 + \sigma_g|\tau| + \tau^2\right)\epsilon_2 \tag{25}$$

$$\bar{M}_3 = \tau\left(3\sigma_g^2 + 4\sigma_g|\tau| + 4\tau^2\right)\epsilon_3 \tag{26}$$

$$\bar{M}_4 = \left(3\sigma_g^4 + 10\sigma_g^2\tau^2 + 9\tau^4\right)\epsilon_4 \quad (27)$$

In Eqs. (21) and (24)–(27), the coefficients in the factors of scale were selected so that the factors of asymmetry could be efficiently represented by sixth order polynomials of the absolute bounded asymmetry. The absolute value functions in these equations are necessary to properly describe fronted peaks, where $\tau<0$.

Eqs. (21) and (24)–(27) are easily evaluated by a programmable calculator or a computer with a spreadsheet program. However, when neither of these tools is available, it may be more convenient to employ simpler, less accurate expressions. The following approximation for the second statistical moment of the EGH is readily evaluated using an arithmetic calculator:

$$\bar{M}_2 \approx \sigma_g^2 + \tau^2 - \frac{\sigma_g|\tau|}{5.577} \quad (28)$$

which is accurate within $\pm 3.04\%$ for all values of σ_g and τ. This approximation is especially useful for the estimation of efficiency N:

$$N = \frac{t_R^2}{\bar{M}_2} \approx \frac{t_R^2}{\sigma_g^2 + \tau^2 - \sigma_g|\tau|/5.577} \quad (29)$$

Eqs. (28) and (29) are also compatible with fronted peaks, where $\tau<0$.

3. Experimental

3.1. Polynomial fits to the factors of asymmetry

Mathematica 3.0 (Wolfram Research, Champaign, IL) was used to approximate numerically the statistical moments of the EGH to an absolute accuracy within $\pm 10^{-15}$. The program numerically calculated the statistical moments for 1025 incremental values of the absolute bounded asymmetry, which ranged from 0 to $\pi/2$, inclusive. For these calculations, the EGH peak height H was set to 1, and the quantities σ_g and τ were constrained by:

$$\sigma_g^2 + \tau^2 = 1 \quad (30)$$

Numerical values for the factors of asymmetry were determined by taking the ratio of the calculated statistical moments to the corresponding factors of scale (based on Eqs. (21) and (24)–(27)). Mathematica was then used to perform relative min-max sixth order polynomial fits on the factors of asymmetry. The numerically calculated values for the second statistical moment were also used in the empirical formulation of Eq. (28).

3.2. Comparing the EGH to the EMG

The EGH was fit to EMG profiles of various asymmetries using Mathematica. The absolute bounded asymmetry of the EMG function was varied from 0 to $\pi/2$, exclusive, in 127 increments, while the peak area and second normalized central moment were both constrained to unity. Each EMG profile was evaluated to an absolute accuracy within $\pm 10^{-15}$ at values between $t_g - 5$ and $t_g + 10$, inclusive, in 1501 increments. EGH functions were then least-squares fit to each set of generated EMG data using the gradient method. The difference between each EMG and corresponding best-fit EGH profile was evaluated by numerically calculating the total residual squared e between the two functions:

$$e \equiv \int_{-\infty}^{\infty} \left(f_{emg}(t) - f_{egh}(t)\right)^2 \, dt \quad (31)$$

3.3. Reagents

The three test compounds are toluene (Fisher Scientific, Fair Lawn, NJ), L-phenylalanine (Sigma Chemical Co., St. Luois, MO), and pyridine (Mallinckrodt Specialty Chemicals Co., Paris, KY). These compounds were chosen due to their various extents of silanol adsorption.

For the analysis of toluene, the mobile phase was a 60:40 mixture of acetonitrile (Optima grade, Fisher Scientific)/purified water (Barnstead Nanopure System, Dubuque, IA). The sample was prepared by dilution of toluene to 0.005% by volume with mobile phase.

For the analysis of phenylalanine, the mobile phase was a 10:90 mixture of acetonitrile/purified water with 0.1% trifluoroacetic acid (Sigma Chemical Co.) and 25 m*M* sodium sulfate (Mallinckrodt Specialty Chemicals Co.). The sample was prepared

Table 1
Polynomial coefficients for approximate factors of asymmetry[a]

ϵ_n	a_0	a_1	a_2	a_3	a_4	a_5	a_6	% error range
ϵ_0	4	−6.293724	9.232834	−11.342910	9.123978	−4.173753	0.827797	±0.06%
ϵ_1	0.75	0.033807	−0.301080	1.200371	−1.813317	1.279318	−0.326582	±0.15%
ϵ_2	1	−0.982254	0.568593	0.512587	−1.184361	0.939222	−0.240814	±0.08%
ϵ_3	0.5	−0.664611	0.706192	−0.293500	−0.083980	0.200306	−0.064264	±0.03%
ϵ_4	1	0.015695	−0.753849	0.578422	0.068108	−0.019288	−0.042403	±0.05%

[a] Let a_i denote the coefficient of the ith order term in the polynomial. The range of relative errors for each polynomial approximation is given in the last column. The corresponding factors of scale are given in Eqs. (21) and (24)–(27).

by making a 1 m*M* solution of phenylalanine in mobile phase.

For the analysis of pyridine, the mobile phase was a 10:90 mixture of acetonitrile/purified water containing 0.025% acetic acid (Fisher Scientific). The sample was prepared by dilution of pyridine to 0.01% by volume with mobile phase.

Each mobile phase was filtered through a 0.2-μm nylon membrane (Alltech, Deerfield, IL) and degassed under vacuum prior to use.

3.4. Chromatographic system

The chromatographic system was assembled with the following components connected respectively in series: Shimadzu LC-600 pump (Kyoto, Japan), Rheodyne 7125 injection port (Cotati, CA), Upchurch Scientific A318 in-line filter (90 nl, Oak Harbor, WA), Keystone Scientific 255-45 reversed-phase column (BDS Hypersil C_{18} 25 cm×4.6 mm, Bellefonte, PA), Hewlett-Packard Series 1050 UV absorption detector (Palo Alto, CA). The external sample loop of the injection port has a sample volume of 10 μl. The semi-micro flow cell of the detector has a void-volume of 1 μl. PEEK tubing of 0.005-in. I.D. (Upchurch Scientific 1535) was used for all connections. To reduce unnecessary back pressure, 0.030-in.-I.D. PEEK tubing (Upchurch Scientific 1533) was used for the waste stream. The detection wavelength was 254 nm for the analysis of toluene and pyridine, and wavelength was 215 nm for the analysis of phenylalanine. The flow-rate was 1 ml/min in all cases.

An Apple Macintosh IIvx equipped with an analog/digital input/output board (National Instruments NB-MIO-16x, Austin, TX) was interfaced with the chromatographic system to collect data. Data-acquisition software was written in-house using LabVIEW 4.1 (National Instruments). The data acquisition rate was 2 Hz.

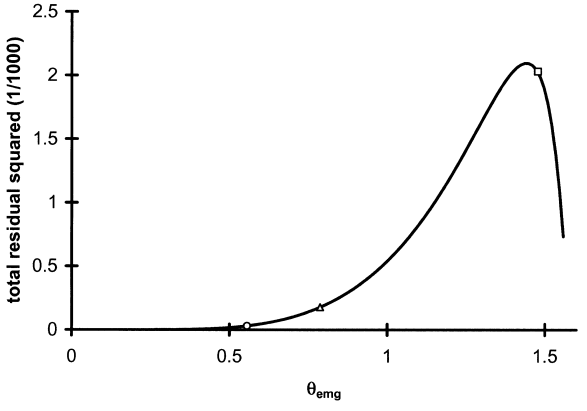

Fig. 3. Total residual squared of EGH fits to EMG functions. The circle, triangle, and square respectively indicate the best-fit EMG asymmetries for toluene, phenylalanine, and pyridine.

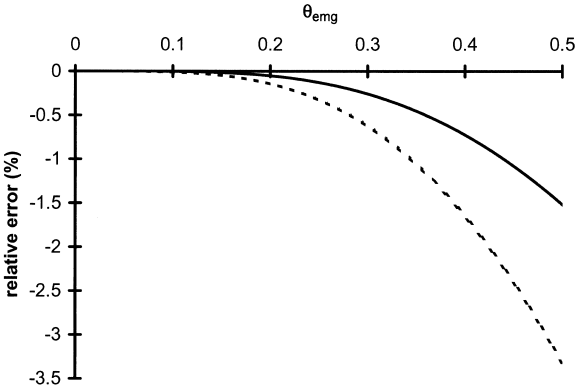

Fig. 4. Relative errors of EGH fits to EMG functions for peak area (solid line) and peak width (dashed line).

3.5. Peak Fitting

The chromatographic peak for each test compound was baseline subtracted and fitted with EMG and EGH functions using in-house software written in LabVIEW 4.1. This software employs the Levenberg–Marquardt method for finding the least-squares regression solution.

3.6. Graphical determination of EGH parameters

The peak maximum for each test compound was determined by fitting a parabola to the 5 data points of greatest ordinate (the tip of the peak that spans 2.5 s). The coordinate of the parabola maximum was then used to establish the peak height and retention time. The asymmetry quantities A_α and B_α were measured using linear interpolation between data points about the ordinate value of 0.15 V. The fraction of height α at which A_α and B_α were measured was calculated by taking the ratio of 0.15 V to the peak height. Eqs. (15) and (16) were then applied to determine the parameters σ_g and τ.

3.7. Comparison of statistical moments

Statistical moments were calculated for the best-fit EMG, best-fit EGH, and graphically determined EGH curves of each test compound. First and higher order EMG moments were calculated using Eqs. (6)–(9). The zeroth moment of the EMG does not need to be calculated because it is a parameter of the EMG function. EGH moments were calculated using Eqs. (21), and (24)–(27) and the corresponding

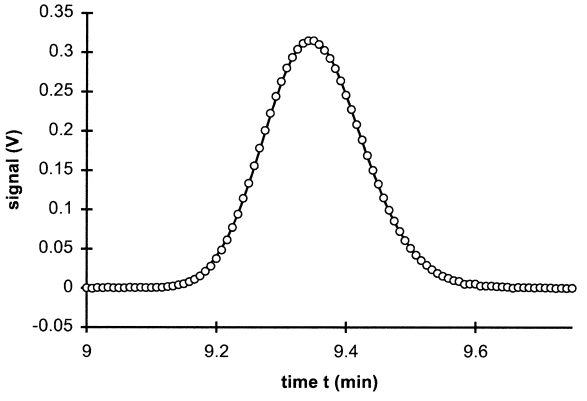

Fig. 5. EMG and EGH Models of the Toluene Peak. The best-fit EMG, best-fit EGH, and graphically determined EGH curves are visually congruent, so they are all represented by a single line. Circles denote chromatographic data points. See Table 2 for parameter values. See text for chromatographic conditions.

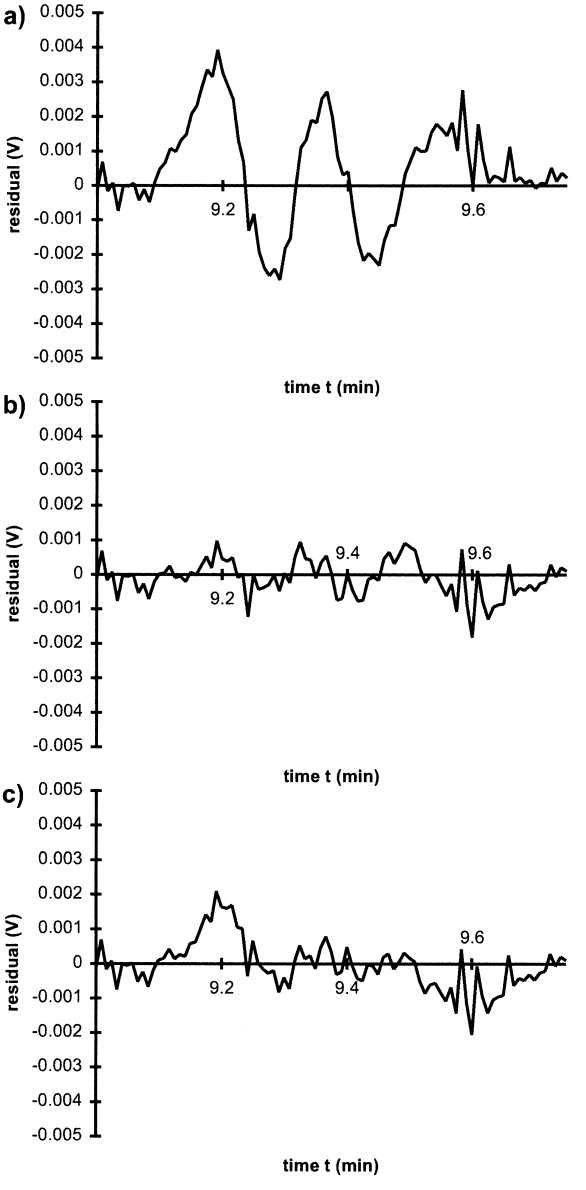

Fig. 6. EMG and EGH Model Residuals for the Toluene Peak. (a) Best-fit EMG model has a mean squared residual of 2.37×10^{-6} V^2. (b) Best-fit EGH model has a mean squared residual of 2.87×10^{-7} V^2. (c) Graphically determined EGH has a mean squared residual of 5.01×10^{-7} V^2. The mean squared noise level of the adjacent baseline is 1.6×10^{-7} V^2.

Table 2
Determined Parameters and Statistical Moments of the Toluene Peak[a]

	Best-fit EMG	Best-fit EGH	Graphically determined EGH	Numerically measured moments	Units
A_α			0.08898		min
B_α			0.09656		min
t_R or t_g	9.312	9.345	9.345		min
H		0.3156	0.3155		V
σ_g	0.06705	0.07590	0.07602		min
τ	0.04163	0.01130	0.01019		min
Mean squared error	23.7	2.87	5.01		10^{-7} V^2
Mean squared noise	1.6				10^{-7} V^2
M_0	0.06058	0.06018	0.06022	0.06025	V min
M_1	9.354	9.353	9.353	9.354	min
M_2	6.229	5.859	5.859	5.962	10^{-3} min^2
M_3	1.443	0.9988	0.8995	1.184	10^{-4} min^3
M_4	1.344	1.058	1.052	1.149	10^{-4} min^4

[a] EMG statistical moments were determined by Eqs. (6)–(9). The measurements of A_α and B_α were taken at the ordinate value of 0.15 V. The graphically determined EGH parameters of σ_g and τ were calculated via Eqs. (15) and (16). EGH statistical moments were determined by Eqs. (21) and (24)–(27).

polynomial approximations for the factors of asymmetry.

The statistical moments for each test compound were measured by trapezoidal-rule numerical integration of chromatographic data using in-house software written in LabVIEW 4.1. The bounds of integration are the same as the bounds of the peak fitting procedure.

4. Results and discussion

4.1. Polynomial fits to the factors of asymmetry

Table 1 shows the polynomial coefficients for the approximations to the factors of asymmetry. Note that the largest relative error is within $\pm 0.15\%$.

Table 3
Determined parameters and statistical moments of the phenylalanine peak[a]

	Best-fit EMG	Best-fit EGH	Graphically determined EGH	Numerically measured moments	Units
A_α			0.1084		min
B_α			0.1391		min
t_R or t_g	7.386	7.429	7.429		min
H		0.4578	0.4599		V
σ_g	0.06514	0.08219	0.08202		min
τ	0.06540	0.02711	0.02742		min
Mean squared error	15.5	1.48	2.02		10^{-6} V^2
Mean squared noise	5.1				10^{-8} V^2
M_0	0.09675	0.09525	0.09551	0.09562	V min
M_1	7.451	7.449	7.450	7.450	min
M_2	8.520	7.308	7.293	7.527	10^{-3} min^2
M_3	5.594	3.049	3.080	3.417	10^{-4} min^3
M_4	3.275	1.814	1.812	1.995	10^{-4} min^4

[a] EMG statistical moments were determined by Eqs. (6)–(9). The measurements of A_α and B_α were taken at the ordinate value of 0.15 V. The graphically determined EGH parameters of σ_g and τ were calculated via Eqs. (15) and (16). EGH statistical moments were determined by Eqs. (21) and (24)–(27).

4.2. Comparing the EGH to the EMG

Fig. 3 shows the total residual squared of EGH fits to EMG functions at various asymmetries. Note that the total residual squared is minute at low asymmetries ($\theta_{emg} < 0.5$), indicating that the EGH can exhibit profiles that are nearly identical to EMG profiles of low asymmetry. The EGH can thus be used as a mathematically simple, numerically stable alternative to the EMG for fitting slightly asymmetric experimental peaks. However, one should be aware that the best-fit parameters τ and σ_g of the EGH function may be different from those of an EMG function. Moreover, since the derivation of the EGH is completely empirical, there is no clear interpretation of the EGH parameters τ and σ_g.

Peak fitting is frequently used to obtain the area or width of an experimental peak. Fig. 4 shows the relative error of the peak area (M_0) and peak width ($\bar{M}_2^{1/2}$) obtained by EGH fits to EMG profiles at low asymmetries. Numerical stability problems of the EMG typically surface for values of $\theta_{emg} < \sim 0.2$ ($\tau/\sigma_g < \sim 0.2$). For $\theta_{emg} < 0.2$, the relative error of the EGH fit is smaller than -0.1% with respect to peak area and smaller than -0.2% with respect to peak width. For $\theta_{emg} < 0.4$, the relative error of the EGH fit is smaller than -1% with respect to peak area and smaller than -2% with respect to peak width.

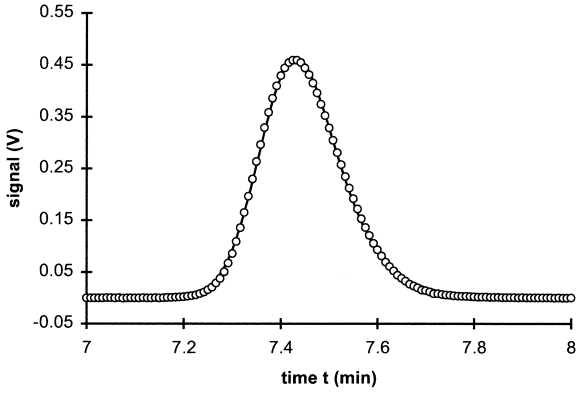

Fig. 7. EMG and EGH Models of the Phenylalanine Peak. The best-fit EMG, best-fit EGH, and graphically determined EGH curves are visually congruent, so they are all represented by a single line. Circles denote chromatographic data points. See Table 3 for parameter values. See text for chromatographic conditions.

4.3. Analysis of the slightly asymmetric toluene peak

The toluene peak has a slight asymmetry that is

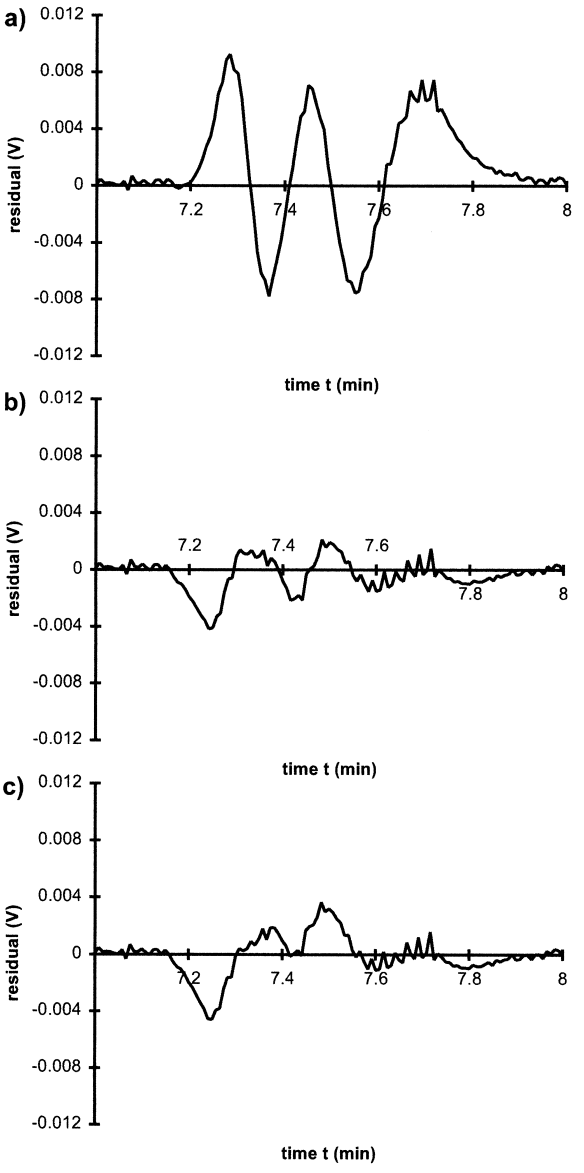

Fig. 8. EMG and EGH Model Residuals of the Phenylalanine Peak. (a) Best-fit EMG model has a mean squared residual of 1.55×10^{-5} V^2. (b) Best-fit EGH model has a mean squared residual of 1.48×10^{-6} V^2. (c) Graphically determined EGH has a mean squared residual of 2.02×10^{-6} V^2. The mean squared noise level of the adjacent baseline is 5.1×10^{-8} V^2.

most likely due to extra-column volumes. According to Fig. 3, the EMG and EGH functions are very similar at this level of asymmetry ($\theta_{emg}=0.56$, $e=3.0\times10^{-5}$, Fig. 3 circle) and should thus produce similar results. The best-fit EMG, best-fit EGH, and graphically determined EGH curves all produce very accurate representations of this peak (Table 2, Figs. 5 and 6). The statistical moments determined for each of these profiles are also in good agreement with each other and with the measured statistical

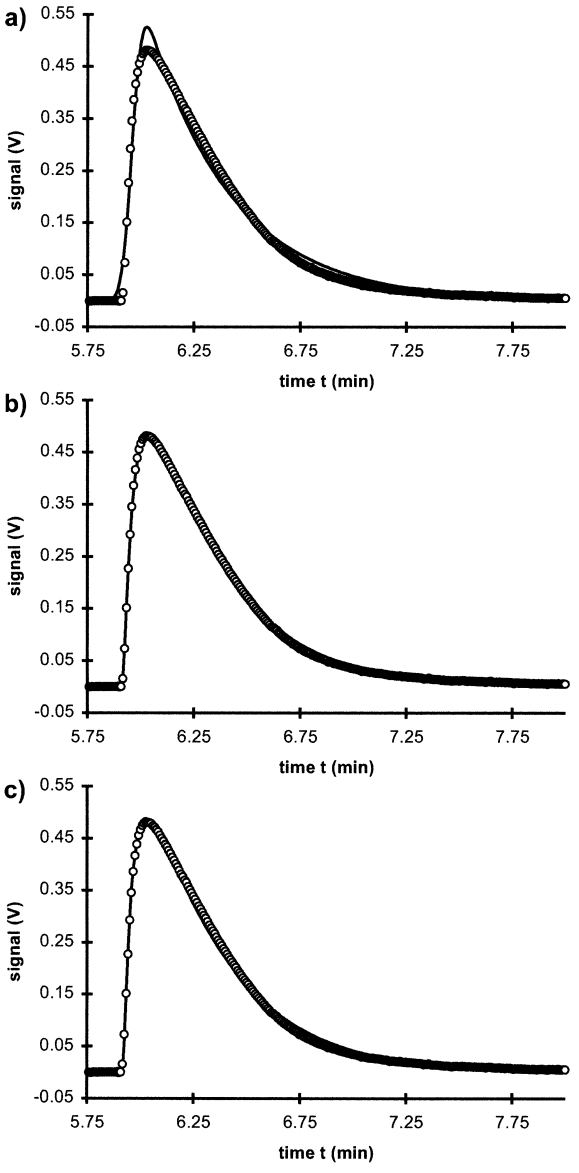

Fig. 9. EMG and EGH Models of the Pyridine Peak. The best-fit EMG (a), best-fit EGH (b), and graphically determined EGH curves (c). Circles denote chromatographic data points. See Table 4 for parameter values. See text for chromatographic conditions.

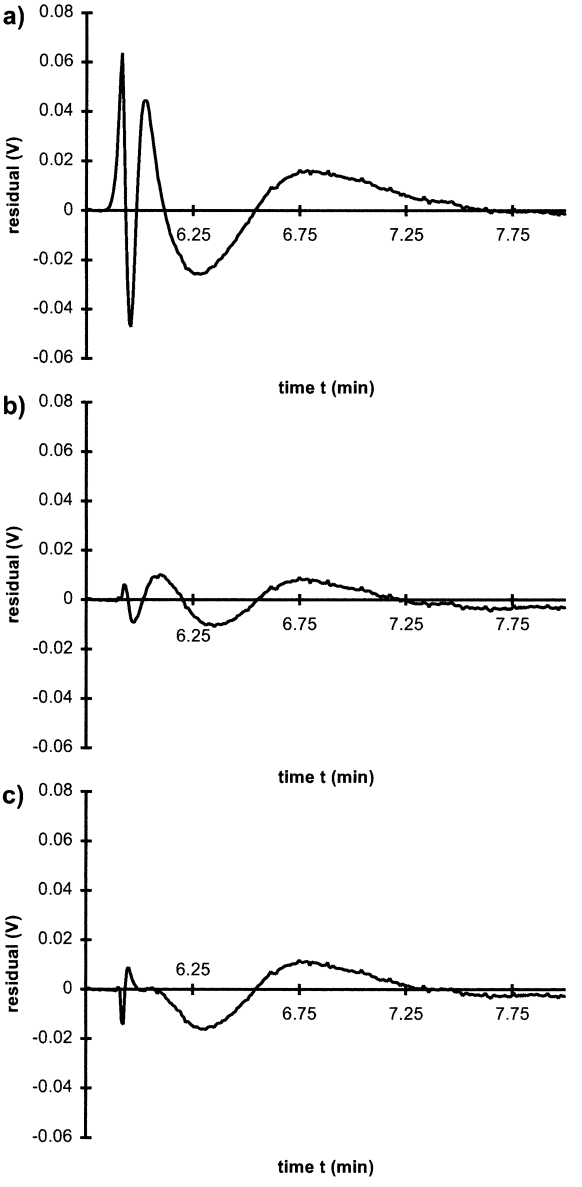

Fig. 10. EMG and EGH Model Residuals of the Pyridine Peak. (a) Best-fit EMG model has a mean squared residual of 2.24×10^{-4} V^2. (b) Best-fit EGH model has a mean squared residual of 2.58×10^{-5} V^2. (c) Graphically determined EGH has a mean squared residual of 4.61×10^{-5} V^2. The mean squared noise level of the adjacent baseline is 2.3×10^{-7} V^2.

moments (Table 2). Deviations from the measured statistical moments become larger at higher orders due to the increasing importance of noise and residuals at distances farther from the peak centroid (M_1) [26].

4.4. Analysis of the moderately asymmetric phenylalanine peak

The phenylalanine peak has a mild asymmetry ($\theta_{emg}=0.79$, $e=1.8\times10^{-4}$, Fig. 3 triangle) due to weak silanol adsorption. The best-fit EMG, best-fit EGH, and graphically determined EGH curves all produce accurate representations of this peak (Table 3, Figs. 7 and 8). Most of the statistical moments determined for each of these profiles are also in good agreement with the measured values (Table 3). The exceptions are the third and fourth moments of the best-fit EMG, which show very large deviations (>60%). This discrepancy is largely due to the increasing importance of residuals at distances farther from the peak centroid.

4.5. Analysis of the highly asymmetric pyridine peak

Because the shape of the EGH and EMG significantly differ from each other at high asymmetries, the EGH may provide a better fit to some of these experimental peaks, such as that of pyridine on a reversed-phase liquid chromatographic system ($\theta_{emg}=1.48$, $e=2.0\times10^{-3}$, Fig. 3 square). Pyridine is commonly used in reversed-phase liquid chromatography to characterize peak tailing caused by silanol adsorption. Fig. 9 shows the pyridine peak modeled by the best-fit EMG, best-fit EGH, and graphically determined EGH curves, and Fig. 10 shows the corresponding residual plots. It is clear that the EGH describes the pyridine peak much better than the EMG does in this particular case. The statistical moments of the best-fit EGH are also in much better agreement with the measured statistical moments than that of the EMG (Table 4).

5. Summary

The EGH function is an empirical model of asymmetric peaks that it is *very easy to implement* due to its mathematical simplicity, numerical stability, and the ease in which its parameters can be related to the graphical representation of the peak. In cases where it may be inconvenient to calculate numerically the statistical moments of an EGH profile, accurate estimates of the moments can be obtained by applying formulae that are easily entered into a spreadsheet program. The EGH can serve as a mathematically simple, numerically stable alternative

Table 4
Determined parameters and statistical moments of the pyridine peak[a]

	Best-fit EMG	Best-fit EGH	Graphically determined EGH	Numerically measured moments	Units
A_α			0.09849		min
B_α			0.5103		min
t_R or t_g	5.959	6.040	6.032		min
H		0.4861	0.4813		V
σ_g	0.03718	0.1513	0.1468		min
τ	0.3978	0.3339	0.3533		min
Mean squared error	22.4	2.58	4.61		10^{-5} V^2
Mean squared noise	2.3				10^{-7} V^2
M_0	0.2579	0.2509	0.2510	0.2505	V min
M_1	6.357	6.328	6.340	6.328	min
$\bar{M}_2$	0.1596	0.1221	0.1339	0.1223	min^2
$\bar{M}_3$	0.1259	0.07880	0.09208	0.07385	min^3
M_4	0.2267	0.1224	0.1502	0.09801	min^4

[a] EMG statistical moments were determined by Eqs. (6)–(9). The measurements of A_α and B_α were taken at the ordinate value of 0.15 V. The graphically determined EGH parameters of σ_g and τ were calculated via Eqs. (15) and (16). EGH statistical moments were determined by Eqs. (21) and (24)–(27).

to the EMG at mild asymmetries since the two functions have very similar shapes in such cases. At higher asymmetries, the EGH may better represent some experimental peak profiles than the EMG. However, its utility in this role is limited since there are several other models of asymmetric peaks that are much more flexible.

The EMG and EGH have complementary advantages and disadvantages. The parameters and statistical moments of the EMG are easily related to each other, but obtaining these quantities requires either approximations [21–25], numerical integration [26], or nonlinear fitting. In contrast, EGH parameters are easily obtained through graphical measurements, but either approximations (Eqs. (21), (24)–(27)) or numerical integration (Eqs. (17)–(19)) are necessary to relate the parameters to the statistical moments.

Acknowledgements

This research was supported by the National Institutes of Health under Grant GM 39515. Kevin Lan was supported by an American Chemical Society Division of Analytical Chemistry Graduate Fellowship sponsored by the Eastman Chemical Company. We thank Glaxo-Wellcome for their donation of the pump and Hewlett-Packard for their donation of the detector.

Appendix A. Derivation of Eqs. (15) and (16)

The EGH function can be restated as:

$$\frac{f_{\mathrm{emg}}(s)}{H} = \exp\left(\frac{-s^2}{2\sigma_g^2 + \tau s}\right) \tag{A.1}$$

where s is the time relative to the retention time, i.e., $t - t_{\mathrm{R}}$. At relative times $-A_\alpha$ and B_α, the EGH profile is at fraction α of peak height, so:

$$\alpha = \exp\left(\frac{-A_\alpha^2}{2\sigma_g^2 - \tau A_\alpha}\right) \tag{A.2}$$

$$\alpha = \exp\left(\frac{-B_\alpha^2}{2\sigma_g^2 + \tau B_\alpha}\right) \tag{A.3}$$

These two equations can be solved for τ and σ_g. Rearrangement of Eq. (A.2) gives us:

$$\tau = \frac{2\sigma_g^2}{A_\alpha} + \frac{A_\alpha}{\ln\alpha} \tag{A.4}$$

Substituting this relationship into Eq. (A.3) yields:

$$\alpha = \exp\left(\frac{-B_\alpha^2}{2\sigma_g^2 + \dfrac{2B_\alpha\sigma_g^2}{A_\alpha} + \dfrac{B_\alpha A_\alpha}{\ln\alpha}}\right) \tag{A.5}$$

Solving this equation for $\sigma_g{}^2$ gives Eq. (15). Substituting Eq. (15) back into Eq. (A.4) produces Eq. (16).

Appendix B. Horizontal scale of an EGH peak

The EGH function can be restated as:

$$\frac{f_{\mathrm{emg}}(t)}{H} = \exp\left(\frac{-\rho^2(t)}{2 + \gamma\rho(t)}\right) \tag{B.1}$$

where:

$$\rho(t) \equiv \frac{t - t_{\mathrm{R}}}{\sigma_g} \tag{B.2}$$

$$\gamma \equiv \frac{\tau}{\sigma_g} \tag{B.3}$$

Based on Eq. (B.2), it is clear that the horizontal scale (peak width) of the EGH peak must be proportional to σ_g at a fixed level of asymmetry γ. Since the level of asymmetry γ is fixed, τ and σ_g must be proportional to each other (Eq. (B.3)). Thus, any expression that is first-order overall with respect to τ and σ_g is proportional to peak width at a fixed level of asymmetry. Furthermore, EGH peaks with time constants τ of opposite sign are simply transposed mirror images of each other and thus have the same peak width. Accordingly, it would be convenient to use instead the absolute value of τ in the first order expressions of peak width.

Appendix C. Factors of scale for higher-order statistical moments

It is commonly known that the standard deviation

σ of a peak increases linearly with the horizontal peak scale; thus, the peak variance $\sigma^2 = \bar{M}_2$ increases with the square of the horizontal peak scale (Eq. (25)). The statistical measures of skew c_3 and kurtosis c_4, which describe peak shape, are known to be invariant with respect to the peak scale [28]:

$$c_3 \equiv \frac{\bar{M}_3}{\sigma^3} \quad \text{(C.1)}$$

$$c_4 \equiv \frac{\bar{M}_4}{\sigma^4} \quad \text{(C.2)}$$

where σ is the standard deviation of the peak. These definitions indicate that the third- and fourth-order moments respectively increase with the third and fourth power of the horizontal peak scale (Eqs. (26) and (27)).

References

[1] L.J. Schmauch, Anal. Chem. 31 (1959) 225.
[2] H.W. Johnson, F.H. Stross, Anal. Chem. 31 (1959) 357.
[3] J.C. Sternberg, in: J.C. Giddings, R.A. Keller (Eds.), Advances in Chromatography, Marcel Dekker, New York, 1966, p. 205.
[4] J.C. Giddings, in: Dynamics of Chromatography,'Principles and Theory', Marcel Dekker, New York, 1965, p. 20.
[5] J.C. Giddings, in: A. Goldup (Ed.), Gas Chromatography, Elsevier Publishing Company, Amsterdam, 1964.
[6] P.T. Kissinger, L.J. Felice, D.J. Miner, C.R. Reddy, R.E. Shoup, in: D.M. Hercules et al. (Ed.), Contemporary Topics in Analytical and Clinical Chemistry, Vol. 2, Plenum Press, New York, 1978, pp. 67–74, 159–175.
[7] M.S. Jeansonne, J.P. Foley, J. Chromatogr. Sci. 29 (1991) 258.
[8] J.P. Foley, J.G. Dorsey, J. Chromatogr. Sci. 22 (1984) 40.
[9] J.R. Torres-Lapasió, J.J. Baeza-Baeza, M.C. García-Alvarez-Coque, Anal. Chem. 69 (1997) 3822.
[10] F. Dondi, A. Betti, G. Blo, C. Bighi, Anal. Chem. 53 (1981) 496.
[11] S. Chesler, S.P. Cram, Anal. Chem. 45 (1973) 1345.
[12] T.S. Buys, K. de Clerk, Anal. Chem. 44 (1972) 1273.
[13] R.D.B. Fraser, E. Suzuki, Anal. Chem. 41 (1969) 37.
[14] J.O. Grimalt, J. Olivé, Anal. Chim. Acta 248 (1991) 59.
[15] A. Berthod, Anal. Chem. 63 (1991) 1879.
[16] R.A. Vaidya, R.D. Hester, J. Chromatogr. 287 (1984) 231.
[17] P.C. Haarhoff, H.J. van der Linde, Anal. Chem. 38 (1966) 573.
[18] D. Hanggi, P.W. Carr, Anal. Chem. 57 (1985) 2394.
[19] P.J. Naish, S. Hartwell, Chromatograpia 26 (1988) 285.
[20] E. Grushka, Anal. Chem. 44 (1972) 1733.
[21] J.P. Foley, J.G. Dorsey, Anal. Chem. 55 (1983) 730.
[22] D.J. Anderson, R.R. Walters, J. Chromatogr. Sci. 22 (1984) 353.
[23] M.S. Jeansonne, J.P. Foley, J. Chromatogr. 594 (1992) 1.
[24] W.E. Barber, P.W. Carr, Anal. Chem. 53 (1981) 1939.
[25] W.W. Yau, Anal. Chem. 49 (1977) 395.
[26] E. Grushka, M.N. Myers, P.D. Schettler, J.C. Giddings, Anal. Chem. 41 (1969) 889.
[27] K. Lan, J.W. Jorgenson, Anal. Chem. 71 (1999) 709.
[28] O. Kempthorne, L. Folks, in: Probability, Statistics and Data Analysis, Iowa State University Press, Ames, Iowa, 1971, p. 20.